

Mitigating Near-field Interference in Laptop Embedded Wireless Transceivers

Marcel Nassar · Kapil Gulati · Marcus R. DeYoung · Brian L. Evans · Keith R. Tinsley

Received: October 23, 2008 / Accepted: date

Abstract In laptop and desktop computers, clocks and busses generate significant radio frequency interference (RFI) for the embedded wireless data transceivers. RFI is well modeled using non-Gaussian impulsive statistics. Data communication transceivers, however, are typically designed under the assumption of additive Gaussian noise and exhibit degradation in communication performance in the presence of RFI. When detecting a signal in additive impulsive noise, Spaulding and Middleton showed a potential improvement in detection of 25 dB at a bit error rate of 10^{-5} when using a Bayesian detector instead of a standard correlation receiver. In this paper, we model RFI using Middleton Class A and Symmetric Alpha Stable ($S\alpha S$) models. The contributions of this paper are to evaluate (1) the performance vs. complexity of parameter estimation algorithms, (2) the closeness of fit of RFI models to the measured interference data from a computer platform, (3) the communication performance vs. computational complexity tradeoffs in receivers designed to mitigate RFI modeled as Class A interference, (4) the communication performance vs. computational complexity tradeoffs in filtering and detections methods to combat RFI modeled as $S\alpha S$ interference, and (5) the approximations to filtering and detection methods developed to mitigate RFI for a computationally efficient implementation.

This research was supported by Intel Corporation.

The work in this paper was presented in part at the 2008 IEEE International Conference on Acoustics, Speech, and Signal Processing.

M. Nassar · K. Gulati · M. R. DeYoung · B. L. Evans
The University of Texas at Austin
Austin, TX - 78712, U.S.A.
Tel.: +1-512-232-1457
E-mail: {nassar, gulati, deyoung, bevans}@ece.utexas.edu

K. R. Tinsley
Intel Corporation
Santa Clara, CA - 95054, U.S.A.
E-mail: keith.r.tinsley@intel.com

Keywords Alpha Stable · RFI Mitigation · Computational Platform · Impulsive Noise · Middleton Noise

1 Introduction

We address the problem of mitigating RFI experienced by the wireless data communication transceivers deployed on a computation platform [1,2]. Table 1 lists several wireless data communication standards and the computing platform subsystems (esp. clocks and busses) that have common spectral occupancy. The interference with wireless transceivers is not only due to the near-field coupling with radiation at frequencies of the driving clocks but also due to the harmonics produced by these subsystems. In [3], the impact of computational platform generated RFI on wireless LAN (WLAN, IEEE 802.11b/g) data communication transceiver was studied. It was shown that computational platform generated RFI may increase the receiver noise floor ten-fold, causing more than 50% loss in range and a significant impact on the throughput performance.

RFI is a combination of independent radiation events and is well modeled using non-Gaussian impulsive statistics. Middleton's Class A, B and C noise models [4] and Symmetric Alpha-Stable ($S\alpha S$) model [5] are perhaps the most common statistical-physical models of RFI. They are well-suited for modeling the predominantly non-Gaussian random process that arises from the nonlinear phenomena that govern electromagnetic interference.

In this paper, we restrict our attention to combating Class A and $S\alpha S$ noise. We evaluate the detection performance of a correlation receiver, a Wiener filter, and Bayes hypothesis testing [6] to mitigate Class A interference. Further, communication performance of the myriad filter [5], the hole puncher filter [7] and the maximum *a posteriori* (MAP) receiver in the presence of additive $S\alpha S$ noise is investigated.

Table 1 Example of computer subsystems interfering with wireless standards [8,9,10]

Standard	Wireless Networking		Interfering Clocks and Busses
Bluetooth	Personal Network	Area	Gigabit Ethernet, PCI Express Bus, LCD clock harmonics
IEEE 802.11b/g	Wireless (Wi-Fi)	LAN	Gigabit Ethernet, PCI Express Bus, LCD clock harmonics
IEEE 802.11n	High-Speed Wireless LAN		Gigabit Ethernet, PCI Express Bus, LCD clock harmonics
IEEE 802.16e	Mobile Broadband (Wi-Max)		PCI Express Bus, LCD clock harmonics
IEEE 802.11a	Wireless (Wi-Fi)	LAN	PCI Express Bus, LCD clock harmonics

Computational complexity vs. communication performance tradeoffs of the filtering and detection methods is evaluated and approximations are proposed for computationally efficient implementation.

The paper is organized as follows. Section 2 gives a brief introduction to Middleton noise models and Symmetric Alpha-Stable models. Section 3 describes different parameter estimation algorithms for these models, and their communication performance vs. computational complexity tradeoffs. Section 4 quantifies the performance of the above methods applied to measured data provided by Intel Corporation. Section 6 describes some RFI combating techniques for Class A and $S\alpha S$ noise. Implementation aspects, results from computer simulations and the communication performance vs. complexity analysis of these algorithms is presented in Section 7, 8, and 9, respectively.

In this paper, “noise” and “interference” are used interchangeably as representing unwanted signals. We developed a MATLAB toolbox (www.ece.utexas.edu/~bevans/projects/rfi/software) that contains implementation of the algorithms mentioned in this paper and can be used to reproduce the obtained results.

2 RFI Modeling

Two general approaches for modeling electromagnetic interference (EMI) are through physical modeling and through statistical-physical modeling. In physical modeling, each source of EMI would require a different circuit model. Statistical-physical models, on the other hand, are independent of the physical conditions and provide accurate universal models for EMI generated from natural and human-made sources. Following are the two key statistical-physical models for RFI.

2.1 Middleton Class A Model

Middleton Class A noise model represents narrowband noise, i.e. when the interference spectrum is narrower than the receiver bandwidth. The Class A model is uniquely determined by the following two parameters [4].

- A is the overlap index. It is the product of the average number of emissions events impinging on the receiver per second and mean duration of a typical interfering source emission, $A \in [10^{-2}, 1]$ in general [11].
- Γ is the ratio of the Gaussian to the non-Gaussian component intensity, $\Gamma \in [10^{-6}, 1]$ in general [11].

The noise statistics for the Middleton Class A model can be expressed as [4]

$$f_Z(z) = e^{-A} \sum_{m=0}^{\infty} \frac{A^m e^{-z^2/2\sigma_m^2}}{m! \sqrt{2\pi\sigma_m^2}} \quad (1)$$

where $\sigma_m^2 = \frac{m}{A+\Gamma}$.

2.2 Symmetric Alpha Stable ($S\alpha S$) Model

The practical applications of the Middleton noise models are limited due to the intractable form of their distributions [4]. Many authors have considered Symmetric Alpha Stable ($S\alpha S$) models as an approximation to Middleton models [12], particularly when noise can be assumed to be broadband and without a Gaussian component. In Section 4, we show that the Symmetric Alpha Stable ($S\alpha S$) model serves as a good approximation for the physical phenomena underlying RFI. A random variable is said to have a $S\alpha S$ distribution if its characteristic function is of the form $\Phi(\omega) = e^{j\delta\omega - \gamma|\omega|^\alpha}$ where

- α is the characteristic exponent. It measures the “thickness” of the tail of the distribution, where $\alpha \in [0, 2]$.
- δ is the localization parameter. It is the median of the $S\alpha S$ distribution and is also equal to the mean when $1 \leq \alpha \leq 2$.
- γ is the scale parameter or the dispersion. It is similar to the variance of the Gaussian distribution, where $\gamma > 0$.

3 Parameter Estimation

In this section, we discuss various parameter estimation algorithms for both Class A and Symmetric Alpha Stable ($S\alpha S$) noise models.

3.1 Middleton Class A Model Parameter Estimation

An efficient parameter estimation method for Class A model has been developed by Zabin and Poor based on the Expectation Maximization (EM) algorithm [11, 13]. They express the

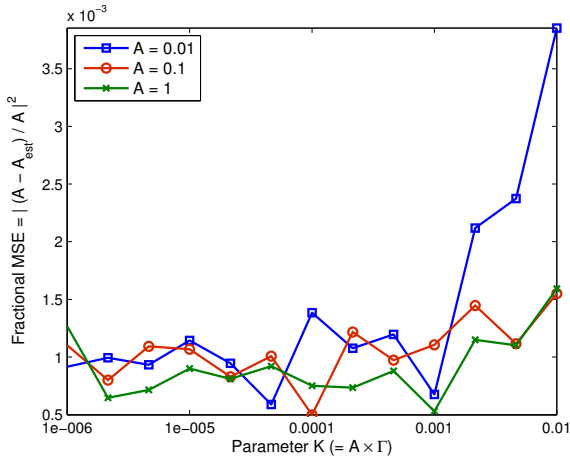


Fig. 1 Fractional MSE in estimates of parameter A using EM algorithm [11] for Class A model.

envelope probability density as a sum of weighted probability densities, under the constraint that the sum of the weights is equal to one. Let $\Theta = (A, K)$, where $K = A \times \Gamma$, denote the parameter set that has to be estimated.

The two steps, the expectation step (E-Step) and the maximization step (M-Step), of the expectation maximization algorithm given in [13] are hence given as follows:

- **E-Step:** Evaluate $Q(\Theta|\Theta^{(p)})$, the expected value of the log-likelihood function
- **M-Step:** Determine $\Theta = \Theta^{(p+1)}$ to maximize $Q(\Theta|\Theta^{(p)})$

Zabin and Poor [11] give a closed form of the log-likelihood function $Q(\Theta|\Theta^{(p)})$. The maximization step is then developed as a two-step iterative procedure [11], where we first maximize over A assuming that K is known and then vice-versa. The first minimization can be expressed as a polynomial of order 2 in A and the second minimization can be expressed as a polynomial of order 4 in K (after the linearizing approximation). The two-step Maximization step can therefore be solved efficiently as it reduces to finding roots to polynomial equations of orders 2 and 4, respectively.

The performance of the EM Estimator developed by Zabin and Poor for Class A model has been shown in Fig. 1 for the estimation of parameter A . The number of iterations taken by the EM estimator to converge is proportional to A and K . The number of iterations was observed to vary between 2 and 30 iterations to converge to a relative error in successive estimates to be less than 10^{-7} in the range of interest. The estimates were calculated using $N = 1000$ envelope data samples which were generated synthetically based on the envelope distribution. Note that the envelope probability density function (pdf) is expressed as an infinite sum and only the first 11 terms were used in simulations. The results were averaged over 50 Monte-Carlo simulation runs.

3.2 Symmetric Alpha Stable (S α S) Parameter Estimation

An efficient, computationally fast estimator was developed by Tsihrintzis and Nikias [12]. It is based on the asymptotic behavior of extreme-order statistics, and is described next.

Let $\mathbf{X} = \{X_1, X_2, \dots, X_N\}$ be a collection of independent realizations of a random variable with the pdf f and cumulative density function (cdf) F . Let X_M and X_m be the maximum and the minimum in the given sequence, respectively. Statistics of X_M and X_m are referred to as extreme-order statistics of the collection. For the alpha-stable model, it can be shown, using the theorem for Feasible Asymptotic Distribution for Extreme-Order Statistics, that the density of maxima and minima (f_M and f_m) approach the Frechet distributions as $N \rightarrow \infty$ [12]. Hence the estimators for the three parameters of the alpha-stable models are given as follows [12].

- Localization Parameter (δ) estimator is given by $\hat{\delta} = \text{median}(X_1, X_2, \dots, X_N)$
- Characteristic Exponent (α) estimator divides the centered data ($= \mathbf{X} - \hat{\delta}$) into L non-overlapping segments of equal length ($= N/L$), calculates the standard deviation \bar{s} and \underline{s} of the sequence $\{\ln(\bar{X}_l)\}$ and $\{-\ln(-\underline{X}_l)\}$, respectively, where $l \in [1, L]$. Here \bar{X}_l and \underline{X}_l are the maximum and minimum of the data segment l , respectively. The estimator for the characteristic exponent is then given by $\hat{\alpha} = \frac{\pi}{2\sqrt{6}} \left(\frac{1}{\bar{s}} + \frac{1}{\underline{s}} \right)$.
- Dispersion (γ) estimator is given by $\hat{\gamma} = \left[\frac{\frac{1}{N} \sum_{k=1}^N |X_k - \hat{\delta}|^p}{C(p, \hat{\alpha})} \right]^{\frac{\hat{\alpha}}{p}}$

where $C(p, \hat{\alpha}) = \frac{1}{\cos(\frac{\pi}{2}p)} \frac{\Gamma(1-\frac{p}{\hat{\alpha}})}{\Gamma(1-p)}$ and p is an arbitrary choice for the order ($0 \leq p \leq \hat{\alpha}/2$) of fractional moment.

The performance of the extreme-order statistics method [12] was observed when setting $\gamma = 5$ (dispersion parameter) and $\delta = 10$ (localization parameter) and by varying α (characteristic exponent) over its entire range ($0 \leq \alpha \leq 2$). Estimates were calculated using $N = 10000$ data samples generated synthetically based on the characteristic function of symmetric alpha stable model. The data was segmented into $L = 1250$ sets for the estimator for the characteristic exponent α . Fractional lower-order moments of $1/3$ were used in the estimator for the dispersion parameter by choosing $p = \hat{\alpha}/3$. The mean square error in the estimates for the characteristic exponent (α) is given in Fig. 2. The results were averaged over 100 Monte-Carlo simulation runs.

4 Measured Data Fitting

Measurements of radio frequency interference (RFI) on a computation platform were obtained from Intel Corporation.

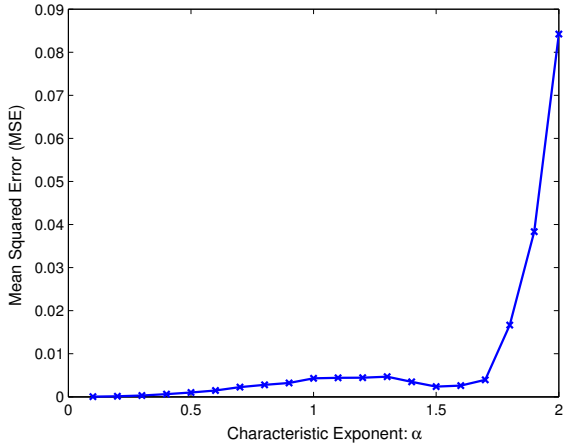


Fig. 2 MSE in the estimates of the characteristic exponent for $N = 10000$ synthetic data samples, true parameters $\delta = 10$ (localization), $\gamma = 5$ (dispersion), $L = 1250$, $p = \alpha/3$.

Measurement data was collected using a 20GSPS scope which represented actual radiated data. Twenty-five sets of measurement data were recorded in different configuration of the computation platform (i.e. different subsystems active etc). The noise was assumed to be broadband, i.e. noise bandwidth was greater than the receiver bandwidth, and the radio was used to listen to the platform noise only (no data communication was being carried out). No further information was provided. For each measurement dataset, 80000 baseband noise samples were used to generate a sample probability density function (pdf) to compare with the estimated Middleton Class A model, symmetric alpha stable model and the Gaussian model. The Kullback-Leibler (KL) divergence [14] is used to quantify the closeness of two probability distribution functions, where a KL divergence of zero indicates an exact match of the densities. The empirical probability density of the measured data was estimated using kernel smoothing density estimators.

We expect the Middleton Class model and the symmetric alpha stable model to approximate the measured data distribution better than the Gaussian model for impulsive noise measurements. Further, the symmetric alpha stable model is expected to provide a closer fit than the Middleton Class A model since the measured RFI is broadband. Fig. 3 compares the KL divergence of distribution of the estimated models from the measured pdf. The measurement sets have been sorted to have increasing KL divergence from the estimated Gaussian model, i.e. increasing impulsiveness of the noise samples. As seen from the figure, both symmetric alpha stable and the Middleton Class A model provide a better approximation to the measured data distribution as compared to the Gaussian model.

Table 2 lists the estimated parameters and the corresponding KL divergence from the measured data distribution for

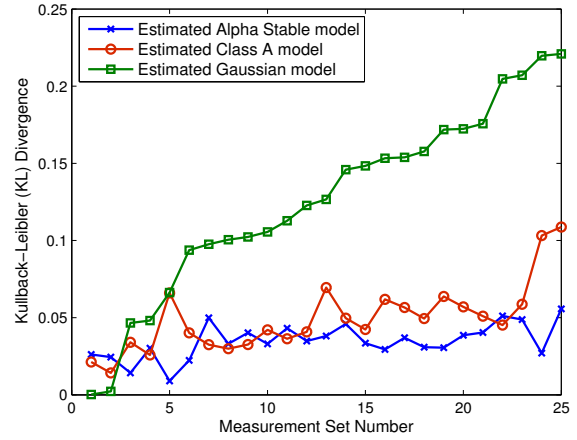


Fig. 3 Kullback-Leibler (KL) divergence of the measured PDF from the estimated symmetric alpha stable PDF, Middleton Class A PDF and an equi-powered Gaussian PDF for twenty-five measured RFI datasets.

Table 2 Estimated model parameters and the corresponding KL divergence from the measured data distribution using symmetric alpha stable ($S\alpha S$), Middleton Class A and Gaussian noise models.

RFI Model	Parameter	Estimated Value	KL Divergence
$S\alpha S$	Localization (δ)	-0.0065	0.0308
	Dispersion (γ)	0.2701	
	Characteristic Exponent (α)	1.4329	
Class A	Overlap Index (A)	0.0854	0.0494
	Gaussian Factor (Γ)	0.6231	
Gaussian	Mean (μ)	0	0.1577
	Variance (σ^2)	1	

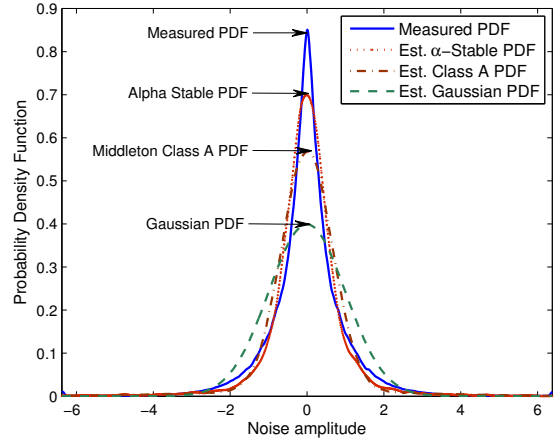


Fig. 4 PDF of measured data compared with the estimated symmetric alpha stable PDF, Middleton Class A PDF and an equi-powered Gaussian PDF. Table 2 lists the estimated parameters for each of the noise model.

a moderately-high impulsive RFI dataset (measurement set 18 in Fig. 3). The KL divergence of the empirical density was computed as 0.0308 from the estimated symmetric alpha stable density, 0.0494 from the estimated Middleton Class A density and 0.1577 from an equi-power Gaussian density. Hence, the measured RFI data was modeled better by the symmetric alpha stable model and the Middleton Class A model as compared to the Gaussian model. The distribution of the measured data, estimated symmetric alpha stable model, Middleton Class A model and the Gaussian model is shown in Fig. 4 to provide a visual justification for the same.

5 System Model

We employ a simple communications model with additive white Gaussian noise replaced by Class A and symmetric α -stable noise. The discrete time received signal is

$$x(n) = \sum_k \sqrt{E_s} s(k) g_{tx}(n - kT) + z(n) \quad (2)$$

where $s(n)$ is a sequence of transmitted symbols, $g_{tx}(\cdot)$ is the sampled pulse shape, E_s is the transmitted signal energy and $z(n)$ is Class A or symmetric α -stable noise. The signal-to-noise ratio (SNR) for Class A noise is defined as $SNR = \frac{E_s}{\sigma_z^2}$, where σ_z^2 is second moment of the noise. On the other hand, since the second order moment of alpha stable processes do not exist, we define the concept of generalized SNR as $GSNR = 10 \log \frac{E_s}{\gamma}$, where γ is the dispersion parameter of $S\alpha S$ process.

Two basic receiver structures are used. For the nonlinear pre-filtering, we first pass the received signal through a nonlinear filter $h_{nl}(\cdot)$, then through a matched filter $g_{rx}(\cdot)$ and into a decision rule $\Lambda(\cdot)$. This receiver model has been studied in the case of zero-memory nonlinearity by Miller and Thomas who motivate it by the fact that it is the structure of a locally optimum detector in additive white noise [15, 6]. The other receiver structure is the standard matched filter $g_{rx}(\cdot)$ followed by a MAP decision rule (Bayes Detection) $\Lambda(\cdot)$ designed for Class A and $S\alpha S$ noise distribution.

For the maximum *a posteriori* (MAP) detector, both Miller [15] and Middleton [6] mention that multiple samples of the received signal provide a method to obtain large performance gains in impulsive noise. Miller assumes a N -path diversity; thus he has N independent versions of the signal. On the other hand, Middleton assumes he has N samples of the received signal, using a fractional sampling approach. In this work, we adopt the approach used by Middleton, although the results can be easily extended to the framework proposed by Miller.

6 Filtering and Detection

After discussing different noise models and evaluating their fit to real data, this section evaluates the detection performance of various detection algorithms that make use of these models. In particular, it starts by discussing the Wiener filter, a linear algorithm, then moves to discussing the optimal Bayes detection (MAP detector). After that it ends by giving two nonlinear preprocessing techniques that can be inserted before the correlation receiver for performance gain as described in Section 5: the myriad filter and the hole puncher.

6.1 Wiener Filtering

The Wiener filter is the optimal linear filter in terms of minimizing the mean-squared error, and a finite impulse response Wiener filter is designed using the famous Wiener-Hopf equations. It assumes that the corrupting noise and the desired signals are wide sense stationary. It is used as a linear filter preceding the correlation receiver (see Section 5).

6.2 Coherent Bayes Detection

Bayes detection is performed by choosing the hypothesis (bit) that maximizes the probability of receiving a signal given the sent hypothesis. Using Class A pdf, Spaulding and Middleton derived the optimal decision rule and its small signal approximation for coherent Class A detection [6].

The Bayes approach to detection is based on hypothesis testing. Spaulding and Middleton considered the case of digital binary signaling (two hypothesis H_1 and H_2) [6]. Using an additive noise model, the optimal Bayesian detection rule for a binary hypothesis case is given by: $\Lambda(\underline{X}) = \frac{p(H_2)p(\underline{X}|H_2)}{p(H_1)p(\underline{X}|H_1)} \underset{\geq H_2}{\overset{< H_1}{>}} 1$ where \underline{X} is the received signal, and $p(\cdot)$ is obtained from Class A pdf.

By taking the Taylor series expansion of the Class A pdf and retaining the first-order terms of the gradient, Spaulding and Middleton were able to obtain a simplified expression for the detection rule, given as

$$x^* = \nabla_{\underline{X}} \ln p_Z(\underline{X}) \cdot \Delta \underline{S} = \sum_{i=1}^N (s_{1i} - s_{2i}) \frac{d}{dx_i} \ln p_Z(x_i) \underset{\geq H_2}{\overset{< H_1}{>}} 0. \quad (3)$$

This formula has a form similar to the standard correlation receiver for Gaussian noise with the exception of the non-linearity $\frac{d}{dx_i} \ln(\cdot)$ that precedes it.

6.3 Myriad Filtering

Myriad filters provide a filtering framework with high statistical efficiency in bell-shaped impulsive distributions like the $S\alpha S$ distribution. Gonzalez and Arce [5] have shown that myriad filters present important optimality properties along the α -stable family. The myriad filter is a sliding window algorithm, that outputs the myriad of the sample window. The myriad of order k of a set of samples x_1, x_2, \dots, x_N is defined as

$$\begin{aligned}\hat{\beta}_k &= \arg \min_{\beta} \sum_{i=1}^N \log[k^2 + (x_i - \beta)^2] \\ &= \arg \min_{\beta} \prod_{i=1}^N [k^2 + (x_i - \beta)^2]\end{aligned}\quad (4)$$

The robustness of this filtering stems from the free-tunable parameter k (*linearity parameter*). This parameter k determines the behavior of the myriad filter: for large k the myriad follows the behavior of a linear estimator, as the value of k decreases the estimator becomes more resilient to impulsive noise. The choice for k can be determined by the following empirical formula $k(\alpha) = \sqrt{\frac{\alpha}{2-\alpha}} \gamma^{\frac{1}{\alpha}}$ where α and γ are the parameters of the $S\alpha S$ noise [5]. It is used as a nonlinear filter preceding the correlation receiver (see Section 5).

6.4 Hole Punching

The algorithm is a nonlinear filter that emulates the functionality of a hard limiter by setting a received sample to zero when it exceeds some threshold value T_{HP} [16,7]. Its functionality can be represented as

$$g_{HP}[n] = \begin{cases} x[n] & |x[n]| \leq T_{hp} \\ 0 & |x[n]| > T_{hp} \end{cases}\quad (5)$$

The intuition is that when a large value is received, we assume it is an impulse and cannot be sure what the true value is. Hole punching works well in impulsive noise, however it does not affect Gaussian noise. The advantage of hole punching is the significantly reduced computational complexity. It is used as a nonlinear filter preceding the correlation receiver (see Section 5).

7 Implementation Aspects

After presenting the theoretical background, this section describes various implementation approaches to the described algorithms. In many cases, direct implementations of the above methods result in high computational complexity. As a result, simpler implementations are given and their performance-complexity tradeoff evaluated in Section 9. In particular, we discuss the Bayesian detection rule and its

small signal approximation and explore the performance of using a lookup table of quantized pdf values and truncated series approximation for Class A noise. In addition to that, we discuss MAP detectors based on ($S\alpha S$) pdf approximation, hole punching, and different implementations of Myriad filtering.

7.1 Class A Bayesian Detection Implementation

The pdf of a Class A random variable is given by an infinite series as given in Section 2.1. This makes direct implementation impossible. However, it is noticed that the latter terms in the series have a diminishing weight ($m!$ in the denominator), that eventually tends to zero as $m \rightarrow \infty$. Thus the pdf can be approximated by truncating the series given by (1), after a certain m . In Section 8, we show the performance of this approximation as the number of truncated terms varies.

On the other hand, a low complexity implementation is given by the form of a look up table. As a result, the problem reduces to quantizing Class A pdf into discrete values, and using those values in the MAP detector. The main premise in this implementation is that the parameters of the Class A model do not vary significantly with time or that the communication performance is not very sensitive to parameter inaccuracies.

7.2 Symmetric α -Stable MAP Detector Implementation

The Symmetric α -Stable random variable does not have a closed form pdf. This complicates the design of the MAP detector, since the pdf has to be approximated using the characteristic function given before in Section 2.2. Many approximations for the Symmetric α -Stable pdf exist but they suffer from numerical instability [17,18]. A well-behaved and computationally tractable approximation was proposed by Kuruoglu [19]. The author shows that we can write a symmetric α -stable random variable as the product of a Gaussian random variable and a positive stable random variable. If we define a normal random variable $X \sim N(0, 2\gamma_x)$ and another, positive stable random variable Y which is independent of X , such that $Y \sim S_{\alpha_x/2}(-1, \cos(\frac{\pi\alpha_x}{4})^{\frac{2}{\alpha_x}}, 0)$, we get a symmetric α -stable random variable $Z = Y^{\frac{1}{2}}X$. Letting $V = Y^{\frac{1}{2}}$, we see that

$$f_Z(z) = \int_{-\infty}^{\infty} f_{Z|V}(z|v) f_V(v) J(z, v) dv \quad (6)$$

$$= \frac{1}{\sqrt{2\pi}} \int_{-\infty}^{\infty} e^{-\frac{z^2}{2v^2}} f_V(v) v^{-1} dv \quad (7)$$

where $J(z, v)$ is the Jacobian of Z with respect to V .

The most pertinent concept in this work is the realization that the pdf $f_Z(z)$ can be sampled uniformly to form a finite

mixture model approximation. The approximation can be written as

$$p_{\alpha,0,\gamma,\mu}(z) = \frac{\sum_{i=1}^N v_i^{-1} e^{-\frac{(z-\mu)^2}{2\gamma v_i^2}} h(v_i)}{\sum_{i=1}^N h(v_i)} \quad (8)$$

where N is the number of components in the mixture.

To generate this pdf, we can take the characteristic function of the Y and evaluate it at N equally spaced points by taking the fast fourier transform (FFT). Finally we compute the finite pdf using the fact that the mixing function $h(v) = 2v f_Y(v^2)$ and plugging it in (8) yielding

$$p_{\alpha,0,\gamma,\mu}(z) = \frac{\sum_{i=1}^N 2e^{-\frac{(z-\mu)^2}{2\gamma v_i^2}} f_Y(v_i^2)}{\sum_{i=1}^N f_Y(v_i^2)}. \quad (9)$$

This pdf approximation forms the basis for an approximation to the MAP detector. A better approximation can be obtained by replacing the uniform sampling by a adaptive optimal sampler that would minimize the squared error.

7.3 Symmetric α -Stable Myriad Filter Implementation

The myriad filter is a constrained optimization problem where the output $\beta \in [x_{min}, x_{max}]$, given that x_{min} and x_{max} are respectively the minimum and maximum value of the data samples in the filtered window. Since the objective function is a polynomial function of β , it is also differentiable in β . By Fermat's theorem, extreme function values are stationary points of the objective function. Using the previous theorem, we propose the following algorithmic implementation of the myriad filter.

1. Expand the polynomial given by (4) in β .
2. Take its derivative by multiplying the coefficients by the appropriate constant according to the corresponding power of β .
3. Root the obtained polynomial and retain the real roots.
4. Evaluate the objective function at the roots and the extremities and output the minimum.

By going through all the stationary points and the extremities we guarantee finding the minimum over the required domain.

A less complex implementation is obtained by restricting our search space just to the samples in the window, ie. $\beta \in \mathcal{S} = \{x_1, x_2, \dots, x_N\}$. This filter is called the Selection myriad filter [20].

8 Simulations

Fig. 5 provides simulation results for a raised cosine pulse (10 samples per symbol period, 10 symbols period per

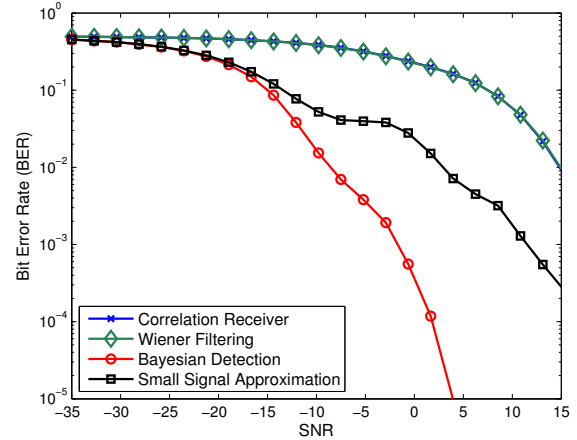


Fig. 5 Communication performance in the presence of Middleton Class A interference with parameters $A = 0.1$ and $\Gamma = 0.5 \times 10^{-2}$.

symbol) sent through a memoryless channel (hence no inter-symbol interference) and corrupted by Middleton Class A interference (with $A = 0.1$ and $\Gamma = 0.5 \times 10^{-2}$). The Wiener filter does not offer much improvement over the correlation receiver since it is a linear filter that is suboptimal in non-Gaussian noise. The improvement in communication performance by using the Bayes detection rule is approximately 25 dB for a bit error rate of 10^{-3} . The small signal approximation performance varies according to the operating SNR. At low SNRs (below -7 dB), a gain of around 20dB is obtained. However, at higher SNRs the small signal approximation fails to achieve the high gains due to the inaccuracy of the Taylor expansion for higher amplitude signals but still maintains a good gain of around 10dB for the higher SNR range (0-15dB). In addition to that, simulations have shown that only relatively few terms (around 3) contribute the most to the communication performance under Class A impulsive noise mitigation.

The performance of the lookup table implementation is given in Fig. 6. As discussed in Section 7.1, the lookup table implementation consists of mainly quantizing the Class A pdf into Q levels. The performance degradation is about 3dB for a 10-level quantization, and only 1dB for a 20-level quantization. As seen later, this method reduces the computational complexity considerably. However, updating table values to parameter changes is more difficult, which makes it more suitable for an implementation in system where the environment does not change rapidly.

Fig. 7 compares the communication performance in the presence of additive S α S noise with $\alpha = 0.9$, $\gamma = 1$, and $\delta = 0$. The myriad filtering is preceded by the parameter estimation for S α S and followed by the correlation receiver. It is observed that the performance of the MAP detector is the best, followed by the myriad filter, hole punching, and then the standard correlation receiver. The performance gap

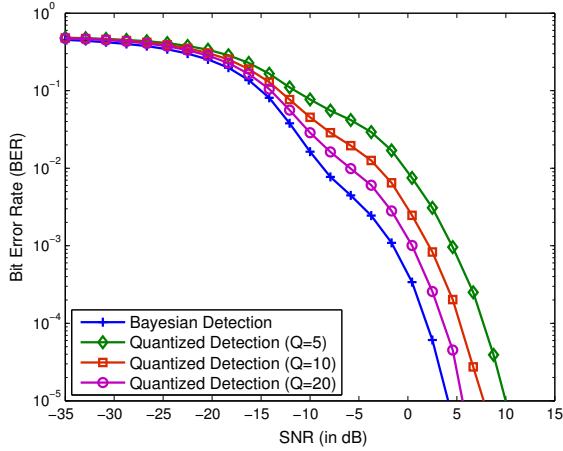


Fig. 6 Communication Performance of the Class A look up table detector with Q quantization levels in the presence of Class A interference with parameters $A = 0.1$ and $\Gamma = 0.5 \times 10^{-2}$.

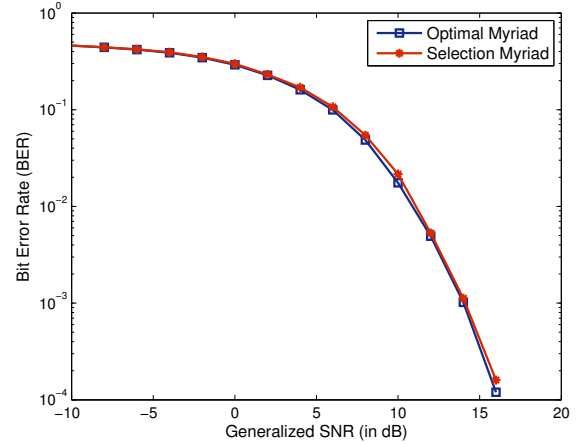


Fig. 8 Performance comparison between the optimal myriad and the selection myriad in the presence of additive $S\alpha S$ noise with parameters $\alpha = 1.5$, $\gamma = 1$, and $\delta = 0$.

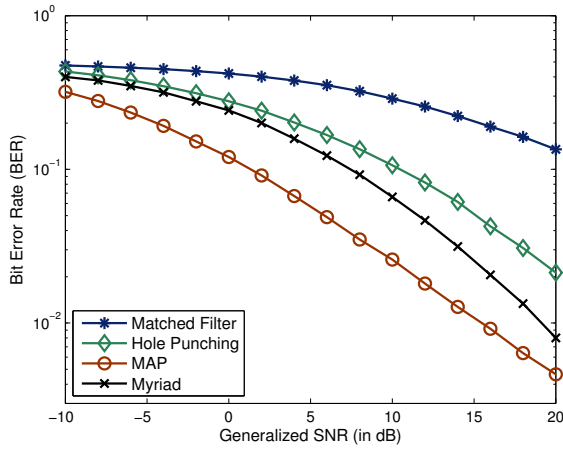


Fig. 7 Communication performance in the presence of additive $S\alpha S$ noise with parameters $\alpha = 0.9$, $\gamma = 1$, and $\delta = 0$.

between the MAP approximation and the myriad filter is around 4dB at a BER of 10^{-1} , while the gap between the myriad and the hole puncher is around 2dB. It is interesting to note that the simple hole puncher performed relatively well compared to the myriad and the correlation receiver. However, this only applies to the 2PAM case. Under higher order modulation techniques, the hole puncher performance suffers from severe degradation.

Fig. 8 shows the communication performance using both the polynomial rooting approach, and the significantly lower complexity selection myriad filter. The polynomial rooting method only provides marginal benefits, as a result the simpler selection myriad is considered as the preferred method of implementation.

Fig. 9 illustrates how the concept of oversampling improves the communication performance under impulsive $S\alpha S$ noise. As N is reduced the performance of the MAP

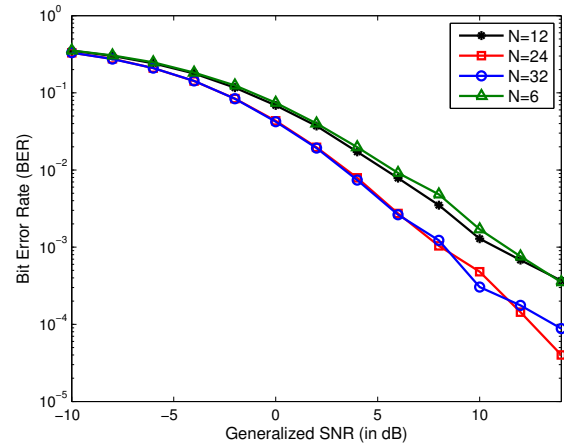


Fig. 9 MAP detector performance with varying the time-bandwidth product (N) in the presence of additive $S\alpha S$ noise with parameters $\alpha = 1.5$, $\gamma = 1$, and $\delta = 0$.

degrades, which agrees with the results obtained by Middleton for the case of Class A noise [6]. However, it should be noted that performance variations are relatively small which will prompt us to use smaller values of N which are more practical to use. As N increases, the sampling rate of the analog to digital converter must increase as well. For large bandwidth signals, this may prove intractable.

9 Complexity vs. Performance Comparison

In this section, we provide a high level analysis of the computational complexity for each of the previous methods, according to the interference type.

Table 3 Complexity vs. performance comparison for Class A noise mitigation algorithms

Method	Computational Complexity	Detection Performance
Bayesian	$\Theta(NMKU)$	High
Small Signal Approx.	$\Theta(NMK)$	High at low SNR
Correlation	$\Theta(M)$	Low
Wiener	$\Theta(MT)$	Low
Look Up Table	$\Theta(ML)$	High

9.1 Class A Noise Mitigation Algorithms

It is expected that the Bayesian detection rule to be the most complex, followed by Wiener filtering, and the correlation receiver, and then the lookup table. To see this, one should observe that the complexity of the Bayesian detection is $\Theta(NMKU)$ operations to perform detection, due to the complex pdf function for Class A noise, where M is the number of samples per symbol, N is the number of terms we retain from the infinite series, U is the cardinality of the signaling space and K is the number of operations required to compute a transcendental function (an exponential in this case). The small signal approximation reduces the complexity to $\Theta(NMK)$. This is because the computation of the nonlinearity in (3) requires $\Theta(NK)$ and it has to be done for M samples. The Wiener filter on the other hand requires $\Theta(MT)$ operations to compute its output, where T is the number of taps of the Wiener filter. The correlation receiver in the given setting only requires $\Theta(M)$ operations. At last, the look up table approach requires $\Theta(L)$ searches, where L is the number of quantization levels, for each of the M samples. This results in a $\Theta(ML)$ complexity. Taking these complexities and the results of Section 8, it is noticed that additional gain comes at the cost of higher complexity. The results are summarized in Table 3.

9.2 Symmetric α -Stable Noise Mitigation Algorithms

The computational complexity per symbol of the simple hole puncher is $\Theta(M)$, where M is the oversampling ratio. This follows from the fact that every sample must be evaluated and a decision made about it. The complexity of the myriad filter depends on the specific implementation. To perform the polynomial rooting approach we need: (a) polynomial expansion (equivalent to a convolution) with complexity $\Theta(MW^2)$, (b) root finding which is equivalent to eigenvalue decomposition of complexity $\Theta(MW^3)$, and (c) W multiplications. Thus the complexity of the polynomial rooting approach is given by $\Theta(MW^3)$. On the other hand, the implementation of the selection myriad requires us to multiply W values for each value and compare them leading to $\Theta(MW^2)$ complexity. The performance difference

Table 4 Complexity vs. performance comparison for symmetric α -Stable noise mitigation algorithms

Method	Computational Complexity	Detection Performance
MAP Approximation	$\Theta(MNS)$	High
Myriad (Optimal)	$\Theta(MW^3)$	Low
Myriad (Selection)	$\Theta(MW^2)$	Low
Hole Puncher	$\Theta(M)$	Low

between these two methods, given in Fig. 8, is minimal which justifies the preference of the less complex selection myriad.

The complexity of the approximate MAP is $\Theta(MNS)$ where N is the number of Gaussian components in the Gaussian mixture used to approximate the $S\alpha S$ distribution, and S is the constellation size. This follows from the fact that we need to sum N weighted exponentials for S times. The results are summarized in Table 4.

10 Conclusion

This paper describes the problem of platform RFI noise that is becoming more relevant as the computational platforms continue to shrink. The paper starts by describing the problem and its relevance in current communication systems. Then it provides a mathematical description of the noise statistics by providing various models that are being used to model this time of noise. After that, the paper gives various algorithms that can be used to estimate the parameters of the mentioned models and goes on to evaluating the accuracy of the given models in fitting real data samples.

After modeling the noise, the paper addresses the question of what can be done to mitigate the effects of impulsive noise. It describes various approaches for both Class A and $S\alpha S$ noise, and analyzes their complexity vs. performance tradeoff. It is noticed that the effects of the impulsive noise can be mitigated by the application of the appropriate methods for both Class A and $S\alpha S$ noise. For Class A noise mitigation, it is observed that the small signal approximation provides the best performance vs. complexity tradeoff at low SNRs. For higher SNR, the MAP detector can be used with a reduced number of terms in the series expansion for reduced computational complexity. On the other hand, the selection myriad filter achieves a good balance between the complexity and performance for $S\alpha S$ noise mitigation. Both of the aforementioned methods are made up of a non-linear filter preceding the standard correlation receiver, which makes them attractive for practical system deployment. It is also noticed that oversampling in the order of 40 samples is enough to achieve considerable gains under impulsive noise.

In conclusion, this paper described computationally tractable methods for mitigating impulsive noise which can have

a substantial impact on current wireless receivers embedded in computational platforms such as laptops and cellphones.

References

1. M. Nassar, K. Gulati, A. K. Sujeeth, N. Aghasadeghi, B. L. Evans, and K. R. Tinsley, "Mitigating near-field interference in laptop embedded wireless transceivers," in *Proc. IEEE Int. Conf. on Acoustics, Speech, and Signal Proc.*, Mar. 30-Apr. 4 2008.
2. K. Gulati, A. Chopra, R. W. Heath, B. L. Evans, K. R. Tinsley, and X. E. Lin, "MIMO receiver design in the presence of radio frequency interference," in *Proc. IEEE Global Comm. Conf.*, Dec 2008.
3. J. Shi, A. Bettner, G. Chinn, K. Slattery, and X. Dong, "A study of platform EMI from LCD panels - impact on wireless, root causes and mitigation methods," *IEEE Int. Symp. on Elec. Comp.*, vol. 3, pp. 626–631, Aug 2006.
4. D. Middleton, "Non-Gaussian noise models in signal processing for telecommunications: New methods and results for class A and class B noise models," *IEEE Trans. on Info. Theory*, vol. 45, no. 4, pp. 1129–1149, 1999.
5. J. G. Gonzalez and G. R. Arce, "Optimality of the myriad filter in practical impulsive-noise environments," *IEEE Trans. on Signal Proc.*, vol. 49, no. 2, pp. 438–441, February 2001.
6. A. Spaulding and D. Middleton, "Optimum reception in an impulsive interference environment-part I: Coherent detection," *IEEE Trans. on Comm.*, vol. 25, no. 9, pp. 910–923, 1977.
7. S. Ambike, J. Ilow, and D. Hatzinakos, "Detection for binary transmission in a mixture of Gaussian noise and impulsive noise modeled as an alpha-stable process," *IEEE Signal Proc. Letters*, vol. 1, pp. 55–57, Mar. 1994.
8. P. Havarasan, M. Haines, H. Skinner, and F. Justice, "Current and future EMI challenges at Intel and how to manage them," *Proc. IEEE Int. Symp. on Elec. Comp.*, vol. 1, pp. 281–283, August 2000.
9. E. A. Morse, "A method for EMI evaluation of notebook computer liquid crystal display panels while eliminating the contribution of computer generated EMI," *Proc. IEEE Int. Symp. on Elec. Comp.*, pp. 343–346, August 1995.
10. T. M. Zeff, T. H. Hubing, J. L. Drewniak, R. E. Dussroff, and T. P. V. Doren, "EMC analysis of an 18" LCD monitor," *Proc. IEEE Int. Symp. on Elec. Comp.*, vol. 1, pp. 169–173, August 2000.
11. S. M. Zabin and H. V. Poor, "Efficient estimation of class A noise parameters via the EM algorithm," *IEEE Trans. on Info. Theory*, vol. 37, no. 1, pp. 60–72, January 1991.
12. G. A. Tsihrintzis and C. L. Nikias, "Fast estimation of the parameters of alpha-stable impulsive interference," *IEEE Trans. on Signal Proc.*, vol. 44, no. 6, pp. 1492–1503, June 1996.
13. J. Bilmes, "A gentle tutorial of the EM [expectation-maximization] algorithm and its application to parameter estimation for Gaussian mixture and hidden markov models," Int. Computer Science Institute, Tech. Rep., 1998.
14. T. M. Cover and J. A. Thomas, *Elements of Information Theory*. Wiley & Sons, New York, 2006.
15. J. Miller and J. Thomas, "Detectors for discrete-time signals in non-Gaussian noise," *IEEE Transactions on Information Theory*, vol. 18, pp. 241–250, Mar. 1972.
16. J. Adlard, T. Tozer, and A. Burr, "Interference rejection in impulsive noise for VLF communications," *IEEE Proc. of Military Comm. Conf.*, vol. 1, pp. 296–300, Nov. 1999.
17. G. Samorodnitsky and M. S. Taqqu, *Stable Non-Gaussian Random Processes: Stochastic Models with Infinite Variance*. Chapman & Hall, 1988.
18. H. Bergstrom, "On some expansions of stable distribution functions," *Arch. Math.*, vol. 2, pp. 375–378, 1952.
19. E. Kuruoglu, "Signal processing in alpha stable environments: A least l_p approach," Ph.D. dissertation, University of Cambridge, 1998.
20. J. Gonzalez, D. Griffith, and G. Arce, "Matched myriad filtering for robust communications," in *Proc. Conf. on Info. Sciences and Systems*, 1996.